CHANGES OF OIL SHALE PORE STRUCTURE AND PERMEABILITY AT DIFFERENT TEMPERATURES

LUSHENG YANG[a,b], DONG YANG[a]*, JING ZHAO[a], ZHENGHE LIU[a], ZHIQIN KANG[a]

[a] Institute of Mining Technology, Taiyuan University of Technology, Taiyuan 030024, P. R. China
[b] College of Arts & Sciences, Shanxi Agricultural University, Jinzhong 030801, P. R. China

Abstract. *While oil shale is heated to a certain temperature, its porous structure undergoes continuous modification and as a result, the rock permeability will also change with increasing temperature. In this paper, the mercury injection apparatus was used for measuring the pore size of oil shale samples at different temperatures. The results showed that, firstly, as the temperature increased, the total pore volume, average pore size and porosity of oil shale increased significantly. When the temperature reached 600 °C, the porosity was increased to 34.6%, making 8.3 times the initial porosity. Secondly, during the heating of oil shale, the volume of mesopores (0.1 μm < d ≤ 1 μm) increased continuously while that of micropores (d ≤ 0.015 μm) decreased. Because the solid organic matter in oil shale was subjected to pyrolysis, micropores began to merge to become medium-sized or mesopores, or even macropores. In the temperature range of 400–500 °C, organic matter was pyrolyzed heavily and both the increment of medium-sized pores percentage and the decline of micropores percentage were very significant. Thirdly, the oil shale permeability increased with rising temperature, being at 600 °C 3.0 × 10^{-8} m^2, which is nearly 600 times that at the room temperature stage of pyrolysis. Shortly, heating oil shale to high temperature can generate new pores and merge the existing ones, which will prompt transforming the tight oil shale into porous rock with high permeability and favour oil and gas seepage.*

Keywords: *oil shale pore structure, permeability, temperature, mercury intrusion method.*

---

* Corresponding author: e-mail *ydscience@hotmail.com*

1. Introduction

Oil shale, also kerogen shale, is a kind of sedimentary rock which is composed of minerals and organic part called kerogen. While it is heated to a certain temperature, the kerogen in it will melt into shale oil or even gasify to oil gas. The shale oil and gas extracted from oil shale by pyrolysis are important energy sources complementary to petroleum and natural gas [1–4]. Since the oil and gas generated by pyrolysis can only migrate through the channels which are formed by connected pores in oil shale, the structure and connectivity of pores directly influence the permeability of the shale, and finally affect the rate of oil and gas productivity [5]. Consequently, these are important study areas of oil shale in-situ recovery. In their study on oil shale samples from Huadian, China, Han et al. [6] used the nitrogen adsorption/ desorption technique to observe changes in the highly porous structure of the rock during combustion. Kang et al. [7] employed the micro-CT scanning technology to study the internal fracturing in Chinese Fushun oil shale at different temperatures, and showed that there was a clear correlation between the amount of cracks formed in the pyrolyzed shale and its permeability. Using the same method Coshell et al. [8] established a positive relationship between bulk density and CT number for Australian oil shale. Tiwari et al. [9] applied micro-CT scanning to investigate the development of internal existing pores and the formation of pore networks before and after pyrolysis of oil shale samples from the Green River Formation in the United States. The researchers found that many pores were formed in oil shale in the pyrolysis process, while its permeability increased from 173 to 2919 d. Zhao et al. [10] used the micro-CT scanning technology to study oil shale samples from Daqing, China for pore structure and permeability changes. Internal porous cracks were found to be well developed along three-dimensional orthogonal surfaces in the shale after high-temperature pyrolysis.

The gas absorption method and micro-CT scanning technology have both been shown in previous studies to be capable of describing the existing pore structure of oil shale. While the former method mainly characterizes nanometer-sized pores, the latter primarily describes micrometer-sized pores and the distribution of pores in three dimensions. In the current study, this mercury intrusion method, which can measure the distribution of the existing pores throughout the whole sample, was used to investigate the porosity, pore distribution and permeability of oil shale at different temperatures.

2. Experimental method

2.1. Experimental equipment

A PoreMaster 33 mercury injection apparatus (Contador Company, USA) was used in the experiment, as shown in Figure 1. The pressure range was

from 1.5 kPa to 231 MPa, and the diameter resolution was 0.007–1000 μm. The system was divided into the low pressure station (1.5 to 350 kPa) and the high pressure station (140 kPa to 231 MPa).

Fig. 1. Mercury injection apparatus.

2.2. Experimental process

The oil shale samples used in the experiment were taken from the Liushuhe Basin, Daqing of China. The oil shale block was processed in a cylinder with a diameter of 7.6 mm and a length of about 20 mm. The results of Fischer assay and proximate analysis of specimens are presented in Table 1. The experiment was to find out the oil shale pore structural evolution as a function of temperature. The temperature in the experiment was set as room temperature (20 °C), 100, 200, 300, 400, 500 and 600 °C. The oil shale specimens were heated in a vacuum muffle furnace to a certain temperature. Each target temperature was held constant for 30 minutes to ensure the pyrolysis reaction was completed, then the heating of the specimens was stopped and they were let cool down to room temperature. Finally, the samples were dried in the oven. After that the mercury intrusion experiment was carried out. During the experiment the test tube was placed in the high pressure chamber, and the mercury intrusion and mercury withdrawal tests

were conducted twice at room temperature (20 °C), 100, 200, 300, 400, 500 and 600 °C. Parameters such as pore volume, porosity and average pore size of three specimens were measured at each temperature.

Table 1. The results of Fischer assay and proximate analysis of oil shale on air-dried basis, wt%

Fischer assay, wt%				Moisture	Ash	Volatile	Fixed carbon
Tar_{ad}	$Water_{ad}$	CR_{ad}	Gas and loss	M_{ad}	A_d	V_d	FC_d
15.02	14.25	62.80	7.93	9.07	28.29	39.06	32.65

Note: $_{ad}$ – on air-dried basis; $_d$ – on dry basis.

3. Pore measurement results and analysis

3.1. Characteristics of pore structure parameters change with temperature

Table 2 presents the values of pore structure parameters of oil shale at different temperatures. Total pore volume is the total volume of pores per unit mass of the test specimen; the total volume of pores and the total intruded mercury volume are equal in value. Median pore size is the pore size when 50% of the mercury has been injected into the test specimen. Porosity is the ratio of the total pore volume to the volume of the test specimen. Table 2 indicates that all the parameters under study increased significantly with increasing temperature. When the temperature was in the range of 400–500 °C, organic matter was pyrolyzed extensively, leaving most pores. When the temperature rose to 600 °C, the values of total pore volume, median and average pore sizes and porosity were 10.7, 10.6, 7.7 and 8.3 times the respective figures at the room temperature stage of the process.

Table 2. Pore structure parameters of oil shale

Temperature, °C	Total pore volume, mL/g	Median pore size, μm	Average pore size, μm	Porosity, %
20	0.0212	0.0266	0.0215	3.72
100	0.0215	0.0283	0.0213	3.78
200	0.0243	0.0550	0.0257	4.28
300	0.0419	0.0637	0.0271	4.63
400	0.0501	0.1100	0.0429	8.76
500	0.1965	0.2212	0.1540	32.55
600	0.2277	0.2825	0.1655	34.64

3.2. Characteristics of different-sized pores at different temperatures

Four pore categories were defined according to the nominal pore diameter, d:

1) micropores d ≤ 0.015 μm;
2) small pores: 0.015 μm < d ≤ 0.1 μm;
3) mesopores: 0.1 μm < d ≤ 1 μm;
4) macropores: d > 1 μm.

The changes in the volume of different-sized pores in oil shale specimens at the tested temperatures were obtained by statistical analysis. The results are given in Table 3 and Figure 2.

From Table 3 it can be seen that the volume of different-sized pores was different as the temperature rose. The volume of macropores increased at first, then decreased above 500 °C. Being minimum, the mesopores volume stayed rather stable up to 300 °C, thereafter began to increase. The volume

Table 3. Distribution of different-sized pores at different temperatures (first mercury intrusion)

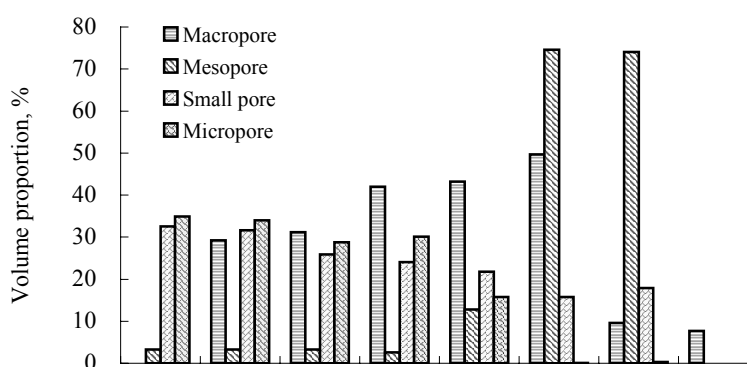| Temperature, °C	Volume of different-sized pores, %			
	Macropores (d > 1 μm)	Mesopores (0.1 μm < d ≤ 1 μm)	Small pores (0.015 μm < d ≤ 0.1 μm)	Micropores (d ≤ 0.015 μm)
20	29.25	3.30	32.55	34.91
100	31.16	3.26	31.63	33.95
200	41.98	3.29	25.93	28.81
300	43.20	2.63	24.11	30.07
400	49.70	12.77	21.76	15.77
500	9.62	74.55	15.78	0.05
600	7.69	74.09	17.92	0.31

Fig. 2. Volumes of different sized pores at different temperatures (first mercury intrusion).

of small pores decreased at temperatures up to 500 °C, then slightly increased when the temperature rose to 600 °C. The micropores volume decreased with increasing temperature. Macropores, small pores and micropores dominated at temperatures from 20 to 300 °C. At 400 °C the distribution of pores underwent a major change. At 500 and 600 °C, mesopores and small pores predominated, accounting for more than 90% of the total pore volume, while the volume of the former was the highest.

Table 2 and Figure 2 indicate a marked change in the internal pore structure of the specimens with increasing temperature. At room temperature, macropores, small pores and micropores were uniformly distributed, each pore group representing about 30% of the total pore volume. The porosity was 3.72%. The proportion of all pores changed when the temperature was increased to 200 °C. The volume of macropores increased to nearly 13% of that at room temperature. The mesopores volume remained practically unchanged, while that of small pores and micropores decreased. In this temperature range, from 20 to 200 °C, free and partially combined water were released from oil shale, causing the formation of more macropores. Some small pores and micropores were connected. At 300 °C, the volume of all four types of pores increased due to the thermal fracturing of minerals in the rock. Pyrolysis of organic matter commenced between 300 and 400 °C, and the volume of macro- and mesopores had increased significantly by 400 °C. In the temperature range of 400–600 °C, the volume of mesopores changed with the progress of the pyrolysis reaction. The micropores were almost connected by this stage. However, the macropores volume decreased significantly because the hydrocarbons released by pyrolysis had not completely migrated from the pore channels, and most of the macropores were blocked.

3.3. Characteristics of pore connectivity in oil shale

In oil shale, some pores are isolated or totally disconnected, but some pores are interconnected to form a kind of network in it. Only interconnected pores can act as channels for migration of oil and gas which are produced in the pyrolysis process. So we defined the interconnected pores as "effective pores". Figure 3 shows the relationships between the cumulative mercury quantity and pore size at 500 °C.

From the two mercury injection withdrawal cycle curves depicted in Figure 3 it can be seen that the first cycle volume of injected mercury was greater than the amount of withdrawn mercury, but all the mercury injected in the second cycle could be completely withdrawn. This was due to the "ink-bottle" effect [11] of the pores. When the mercury was first injected, all the pores were filled with it. When the pressure was released, the mercury in the effective pores could be withdrawn, but the mercury in the "ink-bottle" pores remained. The volume of the withdrawn mercury was therefore the effective pore volume. The volumes and percentages of effective and "ink-bottle" pores at different temperatures are given in Table 4.
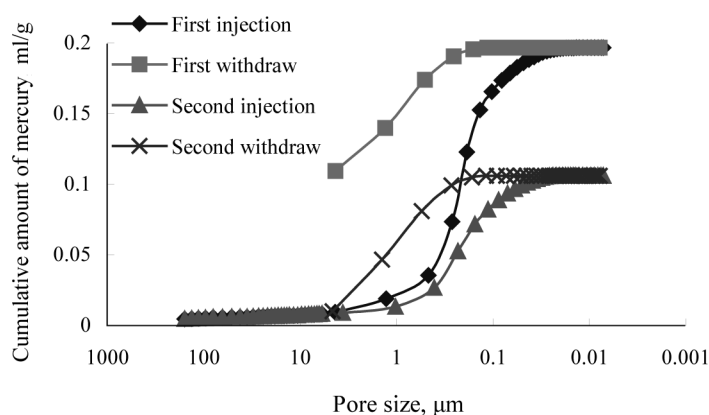
Fig. 3. Relationships between cumulative mercury quantity and pore size at 500 °C.

Table 4. Volumes and percentages of effective and "ink-bottle" pores

T, °C	Volume of effective pores, mL/g	Volume of "ink-bottle" pores, mL/g	Volume proportion of effective pores, %	Volume proportion of "ink-bottle" pores, %	Effective porosity, %	Permeability, 10^{-12} m^2
20	0.0165	0.0047	77.83	22.17	2.95	50.01
100	0.0168	0.0047	78.14	21.86	3.20	50.3
200	0.0192	0.0051	79.01	20.99	3.40	78.94
300	0.0316	0.0103	75.42	24.58	4.04	104.77
400	0.0370	0.0131	73.85	26.15	6.46	470.76
500	0.0942	0.1023	47.94	52.06	15.47	25360
600	0.0945	0.1332	41.50	58.50	14.07	30615

From Table 4 and Figure 4 it can be seen that the volume proportions of both the effective pores and "ink-bottle" pores increased with rising temperature. But comparison shows that changes in the volume percentage of the effective and "ink-bottle" pores are governed by different laws. As the temperature increased, the volume percentage of effective pores increased at first, then decreased, while that of "ink-bottle" pores first decreased, then increased. This indicates that below 200 °C, mainly the connection of existing pores occurred, but as the temperature increased, especially above 300 °C, the main pore evolution process involved the generation of "ink-bottle" pores, while the effective pore volume was observed to increase only slightly.
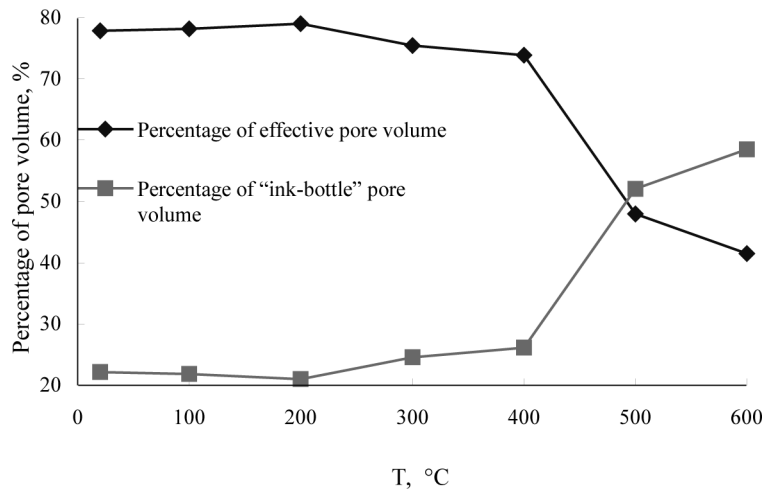
Fig. 4. Pore volume percentage vs temperature.

In the meantime, we can define the effective porosity as the ratio of the total effective pore volume to the volume of the test specimen. The permeability of the sample is calculated using the pore test system of the Master 33 mercury injection apparatus. The results are also presented in Table 4.

The data obtained are illustrated in Figure 5. The figure shows that the effective porosity increased with rising temperature at first and began to decrease above 500 °C. From the figure it can also be seen that the permeability increased gradually with the increase of temperature, but when the temperature was in the range of 400–500 °C, the increment was the most significant. At temperatures up to 600 °C, the permeability was 600 times
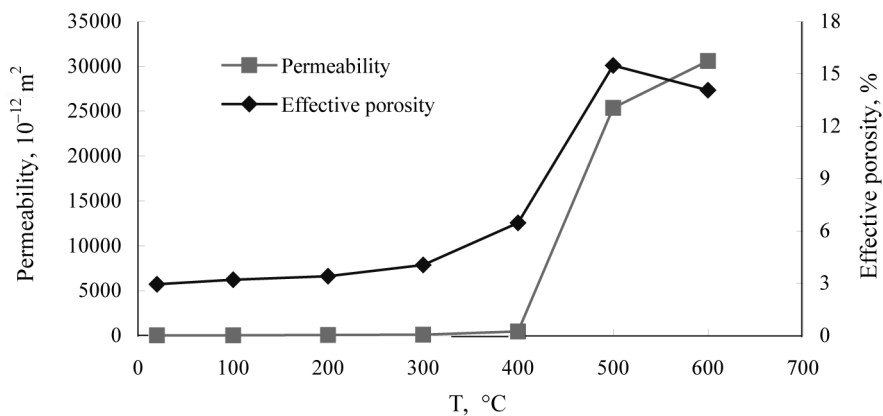

Fig. 5. Effective porosity and permeability vs temperature.

that at room temperature. This is due to the continuous formation and connection of "ink-bottle" pores in oil shale as the temperature increases, which will also increase its permeability.

4. Conclusions

Pore structure measurement experiments on pyrolyzed oil shale were performed at different temperatures. The following conclusions can be drawn:

1) As the temperature rose, the total pore volume, median and average pore sizes and porosity significantly changed. When the temperature was raised to 600 °C, the values of these parameters were 10.7, 10.6, 7.7 and 8.3 times the respective figures at the room temperature stage of the process.

2) When the temperature was below 300 °C, macropores, small pores and micropores dominated in oil shale. Mesopores were few in the temperature range of 20–300 °C. With temperature rising from 300 to 600 °C, the volume of macropores significantly decreased, from 43.2 to 9.62%. The mesopores volume increased noticeably, from 2.63 to 74.55%, and that of small pores decreased from 24.11 to 15.78%. At the same time, there was a sharp decrease in the volume of micropores, from 30.07 to 0.31%.

Especially in the temperature range from 400 to 500 °C, the solid organic matter in oil shale was subjected to extensive pyrolysis, which led to the aggregation and connection of micropores. The volume of mesopores was increased and that of micropores decreased significantly. Therefore, in this temperature range the oil shale pore structure underwent significant modification.

3) Oil shale permeability increased gradually as a function of temperature. At 600 °C, the permeability of oil shale was 3.0×10^{-8} m^2, i.e. nearly 600 times that at the initial stage of pyrolysis.

Shortly, elevating the temperature of oil shale pyrolysis results in the generation of new pores and connection of the existing internal ones in it, which will prompt the transformation of this tight rock into a porous material with high permeability and favour oil and gas seepage.

Acknowledgments

REFERENCES

1. Dyni, J. R. Geology and resources of some world oil-shale deposits. *Oil Shale,* 2003, **20**(3), 193–252.

2. Li, S. Y., Ma, Y., Qian, J. L. Global oil shale research, development and utilization today and an overview of three oil shale symposiums in 2011. *Sino-Global Energy*, 2012, **17**(2), 8–17 (in Chinese).

3. Jiang, X. M., Han, X. X., Cui, Z. G. Study of comprehensive utilization technology of oil shale. *Progress in Nature Science*, 2005, **15**(11), 1342–1345 (in Chinese).

4. Qian, J. L., Wang, J. Q., Li, S. Y. World oil shale utilization and its future. *Journal of Jilin University (Earth Science Edition)*, 2006, **36**(6), 877–887 (in Chinese).

5. Yang, D., Zhao, J., Kang, Z. Q., Zhao, Y. Technology and numerical analysis of in-situ electrical heating on oil shale. *Journal of Liaoning Technical University (Natural Science)*. 2010, **29**(3), 365–368 (in Chinese).

6. Han, X. X., Jiang, X. M., Cui, Z. G. Change of pore structure of oil shale particles during combustion. Part 2. Pore structure of oil-shale ash. *Energ. Fuel.*, 2008, **22**(2), 972–975.

7. Kang, Z. Q., Yang, D., Zhao, Y. S., Hu, Y. Q. Thermal cracking and corresponding permeability of Fushun oil shale. *Oil Shale*, 2011, **28**(2), 273–283.

8. Coshell, L., Mclver, R. G., Chang, R. X-ray computed tomography of Australian oil shales: non-destructive visualization and density determination. *Fuel*, 1994, **73**(8), 1317–1321.

9. Tiwari, P., Deo, M., Lin, C. L., Miller, J. D. Characterization of oil shale pore structure before and after pyrolysis by using X-ray micro CT. *Fuel*, 2013, **107**, 547–554.

10. Zhao, J., Feng, Z. C., Yang, D., Kang, Z. Study on distribution characteristics of pores and fissures inside oil shale under the CT experiment. *Journal of Liaoning Technical University (Natural Science)*, 2013, **32**(8), 1044–1049 (in Chinese).

11. Sun, G. W., Sun, W. J., Jiang, J. Y., Wang, C. H. Experimental study and quantitative characterization of effective porosity in cement-based composite materials. *Industrial Construction*, 2010, **40**(11), 98–101 (in Chinese).